A Theoretical Analysis of Saturation Magnetic Recording

Abstract: A theoretical analysis of the saturation magnetic recording process is presented. The approach is based on the complete characterization of an isolated magnetization transition on the recording surface. The effects of the writing process, demagnetization, recording surface thickness, transducer-to-medium spacing, and readback transducer resolution are considered in calculating the exact pulse shape read back from such an isolated magnetization transition. The theory predicts the significance of each individual parameter that affects the pulse amplitude and resolution of digital recording systems. The theoretical predictions are compared with experimental results measured over a wide range of recording surface properties, and the agreement is excellent. The theory is also in excellent agreement with correlations between magnetic and recording properties that heretofore have been established by experiment alone.

Introduction

In saturation magnetic recording, a bit is defined as a transition in the magnetization of the recording surface. This is to be contrasted to the magnetized region between adjacent transitions which is sometimes also referred to as a bit. In NRZ type recording, the direction of the magnetization of the recording surface is inverted across a transition region. The width and amplitude of the pulse readback from such a transition are among the most fundamental and characteristic parameters of the recording system. For a given transducer and fixed transducerto-medium separation, an explicit dependence of the pulse width and amplitude on the magnetic properties of the recording surface has been experimentally derived. 1-3 In this paper we present a theoretical analysis* of digital recording aimed at deriving the exact dependence of the pulse width and amplitude on the magnetic characteristics of the recording medium, its thickness, the medium-totransducer spacing and the transducer characteristics.

A number of theories have been developed to describe the readback process using a reciprocity theorem.⁴⁻⁸ These are based on the assumption of linearity in the playback process, and they either disregard demagnetization effects or arbitrarily introduce a linear magnetization transition of indeterminate slope. Reciprocity was initially applied to sinusoidal recording, where it does not suffer

In this study we follow an approach similar to that of Miyata and Hartel⁹ to calculate the demagnetization field in the vicinity of an isolated magnetization transition, for a number of different magnetization distributions in the transition region. From this we determine the extent of the transition region after demagnetization, 10 and the role that the write process, the medium thickness, and the magnetic properties of the recording surface play in the resultant magnetization transition. To calculate the readback signal we apply the method of images,11 taking into account the effect of tape thickness, tape-to-transducer spacing, and read transducer losses. Proceeding from ideal to real cases demonstrates the influence of each parameter on the recording process, and allows for independent evaluation of the role of each surface and transducer characteristic property.

Theory

We first derive an expression for the magnetic fields in the vicinity of a single idealized magnetization transition on the recording surface. The calculation is next extended

from the limitations mentioned above. In saturation recording, limited analytical results have been obtained for elementary magnetization transitions and idealized head field functions. These results do not allow for meaningful correlation between magnetic and recording properties, which formed part of our motivation in developing the theory presented in this paper.

As this paper was being prepared, the authors learned that J. Hokkyo, Sony Corp. of Japan, has also performed this theoretical analysis, with similar results. A paper by Hokkyo is to be published.

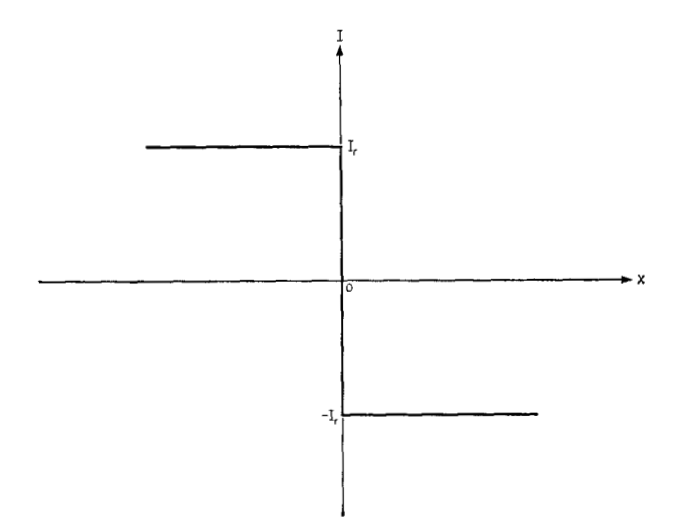
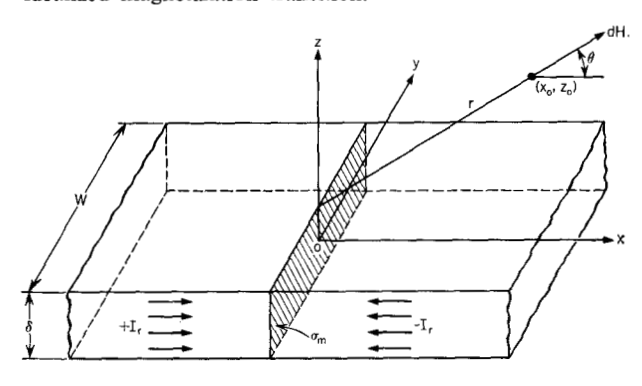


Figure 1 Idealized magnetization transition on a recording surface.

Figure 2 Uniform surface pole density σ_m corresponding to idealized magnetization transition.



to take into account any width of the magnetization transition region. Equating the fields emanating from such magnetization transitions to the coercivity of the recording surface enables one to estimate the width of these transitions and its dependence on the magnetic characteristics of the medium and the writing transducer field gradient.

We next calculate the characteristic pulse read-back from an isolated transition, and relate the pulse width and amplitude to the properties of the medium, the read-back transducer, and the spacing between the transducer and the medium.

• The magnetic field of an idealized magnetization transition

Consider only longitudinal magnetization, independent of the thickness of the medium, and assume the permeability of the recording surface to be that of free space. An idealized transition in the magnetization of the surface is shown in Fig. 1. This discontinuity in the magnetization gives rise to a uniform surface distribution of magnetic poles with density $\sigma_m = 2I_r$, as shown in Fig. 2. Assuming

that $W \gg \delta$, the magnetic field dH of a charge filament $\sigma_m dz$ is (remembering that dH is of opposite sign to I_r)

$$dH = 4\pi \frac{\sigma_m}{2\pi r} dz = \frac{4I_r}{r} dz.$$

Analyzing this into components we have:

$$dH_{z}(x_{0}, z_{0}) = \frac{4I_{r}}{r} dz \cos \theta = 4I_{r} \frac{x_{0}}{x_{0}^{2} + (z_{0} - z)^{2}} dz,$$

$$dH_{\nu}(x_0, z_0) = 0, \quad \text{and} \quad$$

$$dH_z(x_0, z_0) = \frac{4I_r}{r} dz \sin \theta = 4I_r \frac{z_0 - z}{x_0^2 + (z_0 - z)^2} dz.$$

Therefore,

$$H_x(x_0, z_0) = \int_{-\delta/2}^{\delta/2} 4I_r x_0 \frac{dz}{x_0^2 + (z_0 - z)^2}$$

$$= 4I_r \left[\tan^{-1} \frac{z_0 + \delta/2}{x_0} - \tan^{-1} \frac{z_0 - \delta/2}{x_0} \right],$$
(1)

$$H_{\nu}(x_0, z_0) = 0$$
, and (2)

$$H_{z}(x_{0}, z_{0}) = \int_{-\delta/2}^{\delta/2} 4I_{r} \frac{z_{0} - z}{x_{0}^{2} + (z_{0} - z)^{2}} dz$$

$$= 2I_{r} \log \frac{x_{0}^{2} + (z_{0} + \delta/2)^{2}}{x_{0}^{2} + (z_{0} - \delta/2)^{2}}.$$
(3)

The above equations describe the magnetic field of an ideal magnetization transition. If we let $z_0 = 0$, we obtain an expression for the demagnetizing field in the center plane of the medium:

$$H_x(x_0, 0) = 8I_r \tan^{-1} (\delta/2x_0),$$

 $H_y(x_0, 0) = H_z(x_0, 0) = 0.$ (4)

The maximum value of the demagnetizing field occurs at $x_0 = 0$, where

$$H_x(0, 0) = 4\pi I_r. (5)$$

Thus, a demagnetizing factor at the center plane of the recording medium may be defined as

$$N = \frac{H_x(x_0, 0)}{L(x_0, 0)} = 8 \tan^{-1} \frac{\delta}{2x_0},$$
 (6)

which is plotted in Fig. 3. By equating the demagnetizing field to the coercivity of the recording surface, 10 we obtain an expression for the minimum width of the transition region,

$$2x_0 = \delta \cot \frac{H_c}{8I_r} = \delta \cot \left[\frac{\pi}{2} \cdot \frac{H_c}{4\pi I_r} \right], \qquad (7)$$

in terms of the thickness, coercivity, and remanent moment of the surface. This last equation can be used to

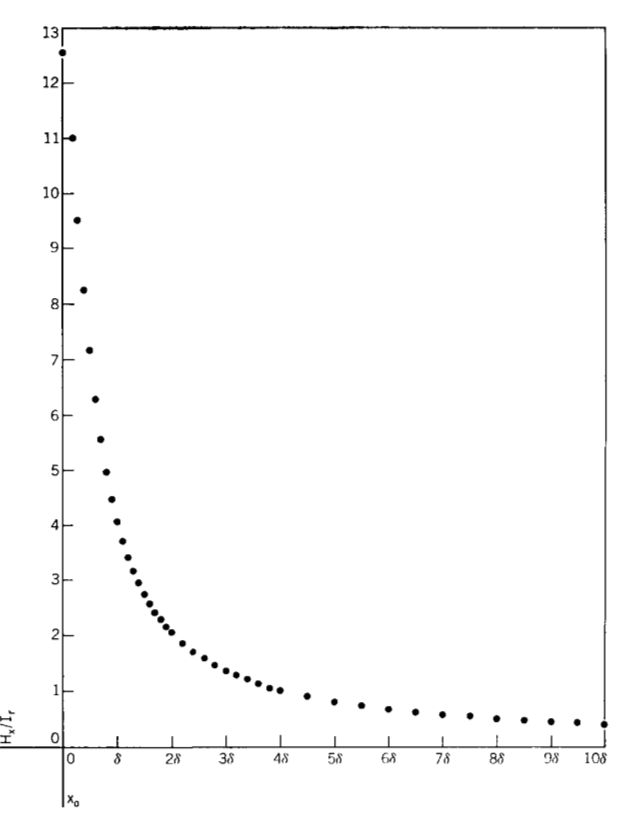


Figure 3 Demagnetizing factor vs x_0/δ for idealized magnetized transition. $H_x/I_r = 8 \tan^{-1} (\delta/2x)$.

calculate the resultant transition region after demagnetization, assuming an ideal writing process which establishes perfect magnetization reversal steps. This situation may be approached in practice by extremely thin recording surfaces with perfectly square hysteresis loop characteristics.

To obtain a more precise definition of the transition region, one must resort to a self-consistent calculation for the field and the magnetization at each point. The convergence of such an approach has been shown, and the results will be reported.

The magnetic field of a magnetization transition of non-zero width

Again assuming only longitudinal magnetization, independent of the thickness of the medium, we consider a transition region as shown in Fig. 4, with a linear variation of the magnetization as shown in Fig. 5. This gives rise to a uniform volume density of magnetic poles,

$$\rho_m = -\nabla \cdot \mathbf{I} = 2I_r/\ell_0$$

Assuming $W \gg \delta$, the field dH of a charge filament along the y-axis is:

$$dH = 4\pi(\rho_m/2\pi r) dx dz = (4I_c/\ell_0 r) dx dz$$
.

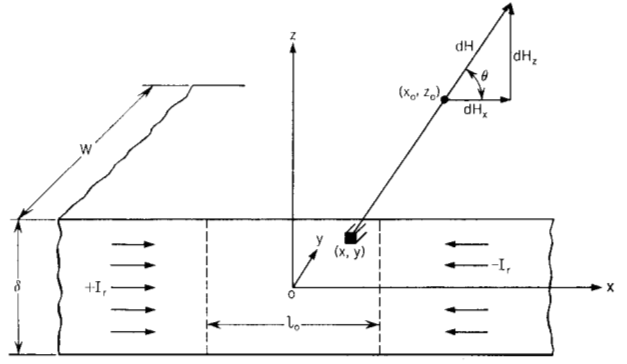
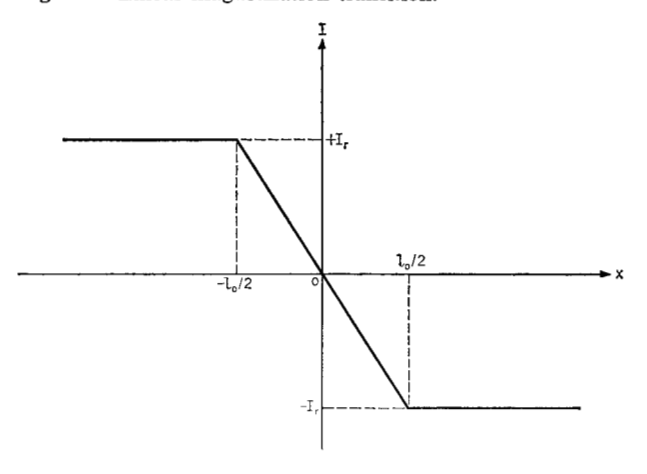


Figure 4 Longitudinal section of recording surface with magnetization transition region ℓ_o ,

Figure 5 Linear magnetization transition.



Analyzing into components we have

 $dH_x(x_0, z_0) = dH \cos \theta$

$$= \frac{4I_r}{\ell_0} \frac{x_0 - x}{(x_0 - x)^2 + (z_0 - z)^2} dx dz,$$

$$dH_y(x_0, z_0) = 0,$$

$$dH_z(x_0, z_0) = dH \sin \theta$$

$$= \frac{4I_r}{\ell_0} \frac{z_0 - z}{(x_0 - x)^2 + (z_0 - z)^2} dx dz.$$

Integrating, we obtain

$$H_{x}(x_{0}, z_{0})$$

$$= \int_{-t_{0}/2}^{t_{0}/2} \int_{-\delta/2}^{\delta/2} \frac{4I_{r}}{\ell_{0}} \frac{x_{0} - x}{(x_{0} - x)^{2} + (z_{0} - z)^{2}} dx dz$$

$$= \frac{2I_{r}}{\ell_{0}} \left[A \log \frac{C^{2} + A^{2}}{D^{2} + A^{2}} + B \log \frac{D^{2} + B^{2}}{C^{2} + B^{2}} + 2C \left(\tan^{-1} \frac{A}{C} - \tan^{-1} \frac{B}{C} \right) + 2D \left(\tan^{-1} \frac{B}{D} - \tan^{-1} \frac{A}{D} \right) \right],$$
(8)

235

where
$$A = z_0 - \frac{\delta}{2}$$
, $C = x_0 - \frac{\ell_0}{2}$,

$$B = z_0 + \frac{\delta}{2}$$
, $D = x_0 + \frac{\ell_0}{2}$,

 $H_x(x_0, z_0)$ is of identical form to $H_x(x_0, z_0)$ but with A and C interchanged and B and D interchanged, and

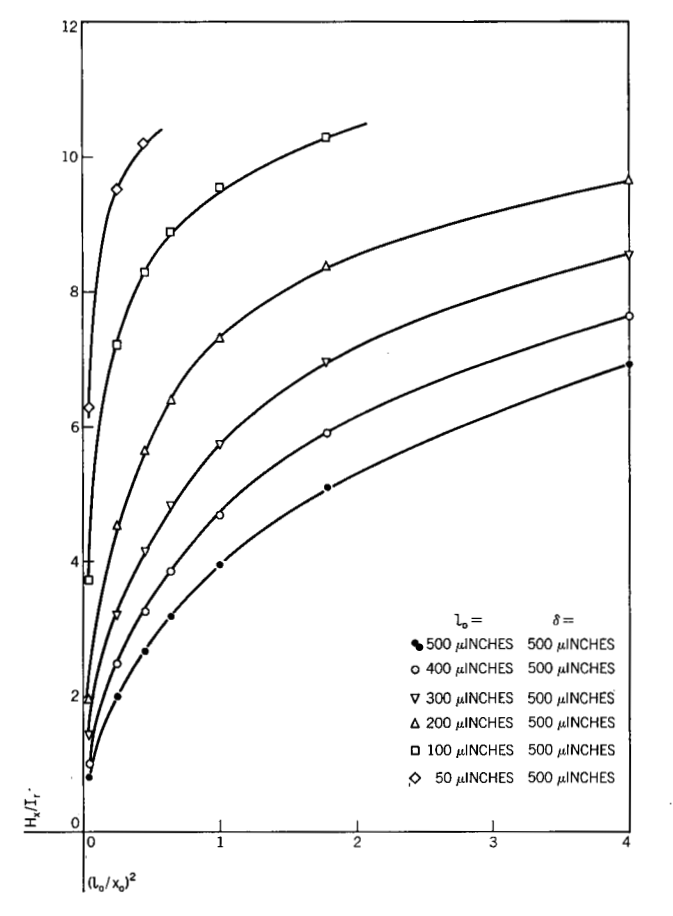
$$H_{\nu}(x_0, z_0) = 0.$$

Evaluating Eq. (8) at $z_0 = 0$ we obtain an expression for the demagnetizing field in the center plane of the medium,

$$H_{x}(x_{0}, 0) = \frac{2I_{\tau}}{\ell_{0}} \left[\delta \log \frac{D^{2} + \delta^{2}/4}{C^{2} + \delta^{2}/4} + 4 \left(D \tan^{-1} \frac{\delta}{2D} - C \tan^{-1} \frac{\delta}{2C} \right) \right]. \quad (9)$$

Thus, an effective demagnetizing factor at the center

Figure 6 The demagnetizing field in a medium 500 microinches thick.

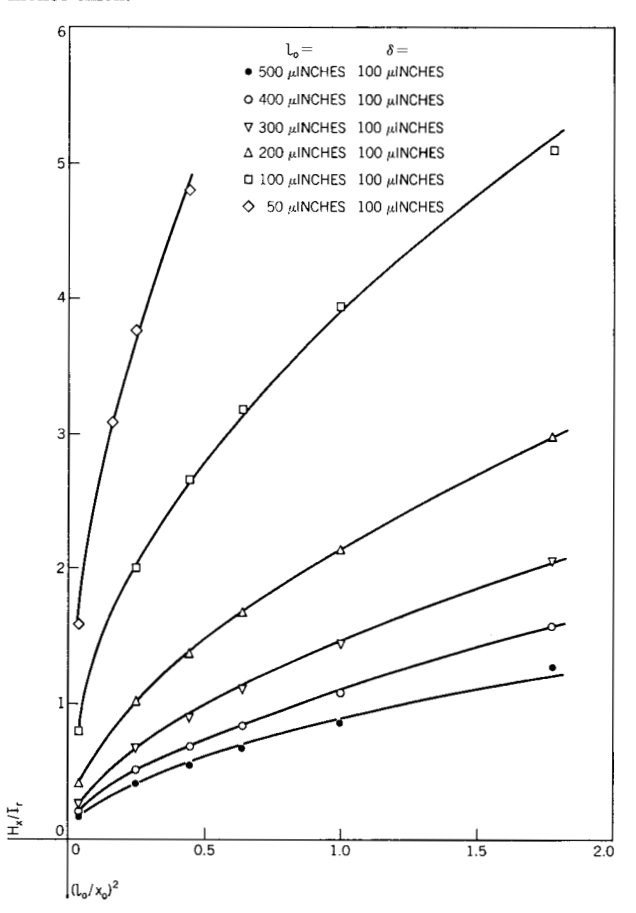


plane of the recording medium and at the end of the transition region may be defined as

$$N = \frac{H_x(x_0, 0)}{I_r} = \frac{2}{\ell_0} \left[\delta \log \frac{D^2 + \delta^2/4}{C^2 + \delta^2/4} + 4 \left(D \tan^{-1} \frac{\delta}{2D} - C \tan^{-1} \frac{\delta}{2C} \right) \right].$$
(10)

Equation (10) is plotted in Figs. 6, 7, and 8 as a function of $(\ell_0/x_0)^2$ for three different values of δ , and with ℓ_0 as a parameter. The thicknesses of 500 and 100 microinches represent approximately the upper and lower limits, respectively, of typical particulate recording surfaces, while the thickness of 10 microinches is representative of metallic surfaces. If H_x is set equal to the coercivity of the surface, we can obtain from Eq. (10) the value of the resultant transition region $2x_0$ in terms of the length of the written transition ℓ_0 , the thickness δ , and the magnetic parameters of the surface H_c/I_r . The results are tabulated in Tables 1, 2 and 3 for the three different

Figure 7 The demagnetizing field in a medium 100 microinches thick.



thicknesses and for several values of the H_c/I_r ratio. It is quite clear from these results that the writing process which determines the initial transition ℓ_0 , has only a very minor effect on the resultant transition $2x_0$. To obtain a realistic value of ℓ_0 , one must know the writing transducer field gradient and the slope of the sides of the hysteresis loop of the recording surface. Such estimates give values of ℓ_0 which correspond to the smallest of those assumed in Tables 1, 2 and 3, thus strengthening the argument that the writing process is not critical at all. Again, for a more precise determination of the transition region, a self-consistent calculation for the field and the magnetization at each point is required.

To determine explicitly the effect of the thickness δ on the demagnetization, Eq. (10) is plotted for several values of δ , as shown in Fig. 9. It is quite clear that the demagnetizing field depends linearly on the thickness for the range of parameters shown in Fig. 9. Furthermore, for values of H_c/I_r between 0.2 and 1, which are representative for chemically deposited recording surfaces, we deduce from Fig. 9 that,

$$H_e/I_r \propto \delta(\ell_0/x_0)^2$$
, and
 $x_0 \propto (I_r \delta/H_e)^{1/2}$. (11)

Therefore, the resultant transition region in thin recording surfaces is primarily determined by surface demagnetization, and is proportional to the square root of the ratio $I_{\tau}\delta/H_c$. The same dependence also holds approximately for thick surfaces (see Figs. 6 and 7). Of course it is evident that the exponent which defines the dependence of the transition region on the magnetic properties and the thickness of the recording surface is a function of ℓ_0 , decreasing as ℓ_0 increases.

However, the curves shown in Figs. 6-9 tend to become parabolic or even of higher order, for small values of $H_{\rm z}/I_{\rm r}$ or for large recording surface thicknesses. Consequently, the dependence of the resultant transition region on the magnetic properties and the thickness of the recording surface, should more appropriately be described as

$$x_0 \propto \left(\frac{I_r \delta}{H_c}\right)^n$$

where the exponent n is very nearly 1/2 for the thinner recording surfaces with typical parameters, but gradually becomes larger than 1/2—and conceivably larger than 1—for surfaces with very large thickness and/or remanence, and with very low coercivity. Therefore, to the extent that the spread of the magnetization transition affects the readback pulse width, the magnetic properties and the thickness of the recording surface will affect the resolution of the recording system in a form similar to Eq. (11).

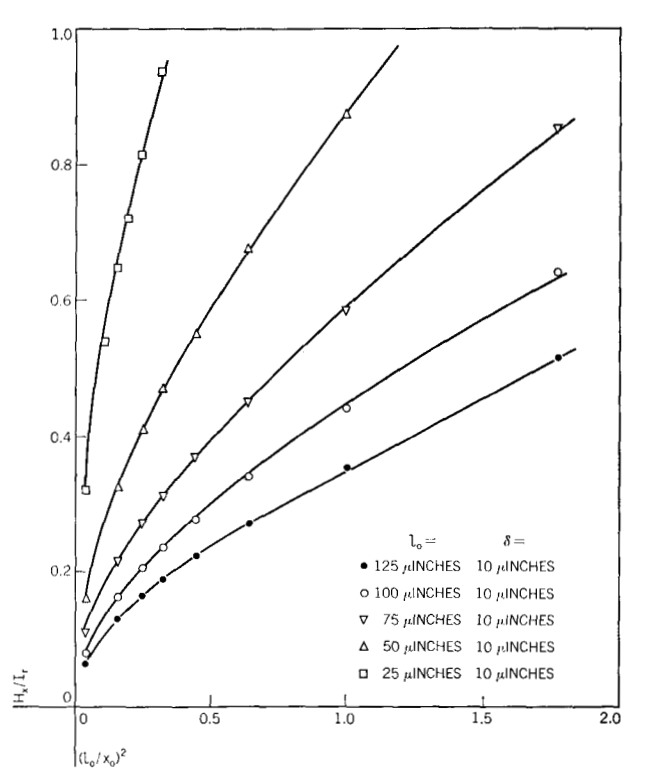


Figure 8 The demagnetizing field in a medium 10 micro-inches thick.

Figure 9 Demagnetizing field in thin media of various thicknesses.

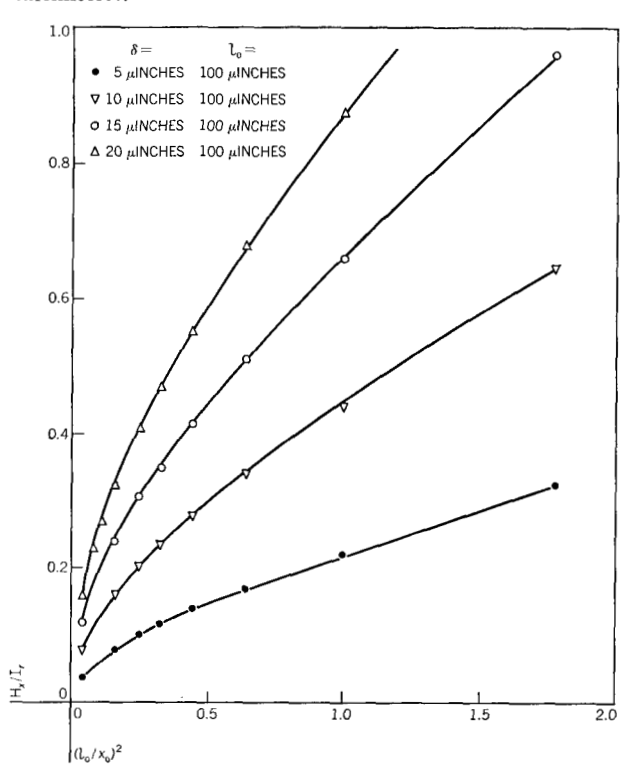


Table 1 Surface thickness at $\delta = 500 \mu in$.

H _o /I _r (Oe-cm³/emu)	Written transition, ℓ₀(µin.)	Resultant transition, $2x_0(\mu in.)$
3.5	500	1136
	400	1096
	300	1072
	200	1000
	100	1050
6	500	588
	400	580
	300	558
	200	544
	100	500
8	500	500
	400	400
	300	334
	200	324
	100	316

Table 2 Surface thickness at $\delta = 100 \mu in$.

H _o /I _r (Oe-cm³/emu)	Written transition, $\ell_0(\mu in.)$	Resultant transition, $2x_0(\mu in.)$
1	500	884
	400	858
	300	832
	200	816
	100	756
	50	744
2	500	580
	400	512
	300	458
	200	422
	100	400
	50	390
3.5	500	500
	400	400
	300	312
	200	256
	100	225
	50	212
4.5	500	500
	400	400
	300	300
	200	210
	100	171
	50	162

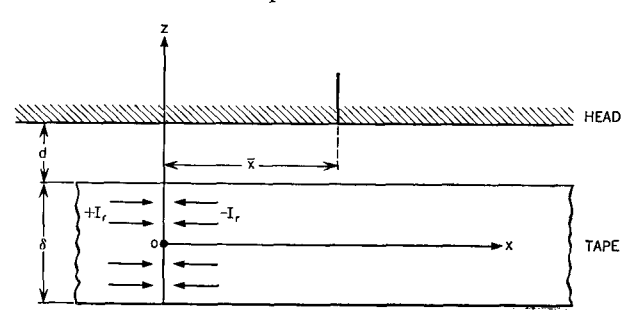
• The reproduced pulse by an ideal head for idealized magnetization transition

Consider an idealized playback head consisting of a semi-infinite block of high permeability material spaced a distance d above the recording surface, as shown in Fig. 10. Assuming the head surface to be an equipotential, by the method of images we obtain the field entering the

Table 3 Surface thickness at $\delta = 10 \mu in$.

H_c/I_r (Oe-cm 3 /emu)	W ritten transition, $\ell_0(\mu in.)$	Resultant transition, $2x_0(\mu in.)$
0.5	25	158
	50	164
	75	171
	100	180
	125	189

Figure 10 Recording surface with idealized magnetization transition and idealized reproduce head.



head in terms of the field of the recording surface in the absence of the head,

$$B_z(x, d + \delta/2) = [2\mu/(\mu + 1)]H_z(x, d + \delta/2),$$

where μ is the head permeability and H_z is given by Eq. (3). Therefore,

$$B_z(x, d + \delta/2) = \frac{4\mu}{\mu + 1} I_r \log \frac{x^2 + (d + \delta)^2}{x^2 + d^2},$$
 (12)

and the flux entering the head is

$$d\Phi = \frac{4\mu}{\mu + 1} I_r W \log \frac{x^2 + (d + \delta)^2}{x^2 + d^2} dx.$$

Consequently,

$$\Phi = \int_0^z d\Phi$$

$$= \frac{4\mu}{\mu + 1} I_r W \left[\bar{x} \log \frac{\bar{x}^2 + (d + \delta)^2}{\bar{x}^2 + d^2} + 2(d + \delta) \tan^{-1} \frac{\bar{x}}{d + \delta} - 2d \tan^{-1} \frac{\bar{x}}{d} \right]. \quad (13)$$

The voltage readback will be proportional to the time rate of change of the flux Φ , and the number of turns N of the read-back transducer,

$$e(\bar{x}) = -N \frac{d\Phi}{dt} \times 10^{-8} = -N \frac{d\Phi}{d\bar{x}} \frac{d\bar{x}}{dt} \times 10^{-8}$$
$$= (-Nv \times 10^{-8}) \frac{d\Phi}{d\bar{x}},$$

where v is the velocity of the surface with respect to the reproduce head in cm/sec.

Differentiating Eq. (13) we have

$$e(\bar{x}) = \left[Nv W(I_r \times 10^{-8}) \frac{4\mu}{\mu + 1} \right]$$

$$\log \frac{\bar{x}^2 + (d + \delta)^2}{\bar{x}^2 + d^2},$$
(14)

and this agrees with the result of the reciprocity theory for this idealized case. Of course, Eq. (14) can be obtained directly from Eq. (12) without having to calculate the flux first, since

$$\frac{d}{dq}\int_{p}^{q}f(x)\ dx = f(q).$$

It is interesting to note that one may obtain the same expression as Eq. (14) by integrating the x component of the flux with respect to z between the limits $d + \delta/2$ and ∞ .

The maximum value of the voltage occurs at $\bar{x} = 0$, where

$$e_{\text{max}} = e(0) = \left[Nv W(I_r \times 10^{-8}) \frac{8\mu}{\mu + 1} \right] \log \frac{d + \delta}{d}.$$
 (15)

The pulse width at q per cent of peak amplitude is given by 9

$$(P.W.)_q = 2x_q = 2\sqrt{\frac{(d+\delta)^2 - C_q d^2}{C_q - 1}},$$
 (16)

where

$$C_q = \left(\frac{d+\delta}{d}\right)^{0.02q}$$

and x_q is the position where the amplitude has dropped to q per cent of its maximum value.

Therefore, the half pulse width is

$$(P.W.)_{50} = 2\sqrt{(d+\delta)d}.$$
 (17)

• The reproduced pulse by an ideal head for a magnetization transition of non-zero width

The magnetic field of an isolated magnetization transition of nonzero width is given by Eq. (8), which is quite lengthy. Instead we resort to a magnetization transition of the form suggested by Miyata and Hartel,⁹

$$I_x = -\frac{2}{\pi} I_r \tan^{-1} \frac{x}{a} ,$$

which gives rise to a volume density of magnetic charge

$$\rho = \frac{2}{\pi} I_r \frac{a}{a^2 + x^2}.$$

Following exactly the same procedure as in deriving Eq. (8), except that integration over x is now between the limits $-\infty$ to $+\infty$, we obtain, outside the recording medium,

$$H_{x}(x_{0}, z_{0}) = 4I_{r} \left[\tan^{-1} \frac{z_{0} + \delta/2 + a}{x_{0}} - \tan^{-1} \frac{z_{0} - \delta/2 + a}{x_{0}} \right], \quad (18)$$

$$H_{\nu}(x_0, z_0) = 0$$
, and (19)

$$H_s(x_0, z_0) = 2I_r \log \frac{x_0^2 + (z_0 + \delta/2 + a)^2}{x_0^2 + (z_0 - \delta/2 + a)^2}.$$
 (20)

The similarity of Eqs. (18), (19), and (20) to Eqs. (1), (2), and (3) is apparent. Therefore, by analogy to Eq. (12) the flux density at the head surface becomes

$$B_z\left(x, d + \frac{\delta}{2}\right) = \frac{4\mu}{\mu + 1} I_r \log \frac{x^2 + (d + \delta + a)^2}{x^2 + (d + a)^2},$$
(21)

and the flux entering the idealized head is, by analogy to Eq. (13),

$$\Phi = \frac{4\mu}{\mu + 1} I_r W \left[\bar{x} \log \frac{\bar{x}^2 + (d + \delta + a)^2}{\bar{x}^2 + (d + a)^2} + 2(d + \delta + a) \tan^{-1} \frac{\bar{x}}{d + \delta + a} - 2(d + a) \tan^{-1} \frac{\bar{x}}{d + a} \right].$$
 (22)

Differentiating Eq. (22) we obtain, for the voltage read back,

$$e(\bar{x}) = \left[Nv W(I_r \times 10^{-8}) \frac{4\mu}{\mu + 1} \right] \times \log \frac{\bar{x}^2 + (d + \delta + a)^2}{\bar{x}^2 + (d + a)^2},$$
 (23)

which has a maximum value ($\bar{x} = 0$) of

$$e_{\text{max}} = e(0) = \left[Nv W(I_r \times 10^{-8}) \frac{8\mu}{\mu + 1} \right]$$

$$\times \log \frac{d + \delta + a}{d + a}, \qquad (24)$$

and a pulse width, at q per cent of peak amplitude, of

$$(P.W.)_q = 2x_q = 2\sqrt{\frac{(d+\delta+a)^2 - C_q(d+a)^2}{C_q - 1}},$$
(25)

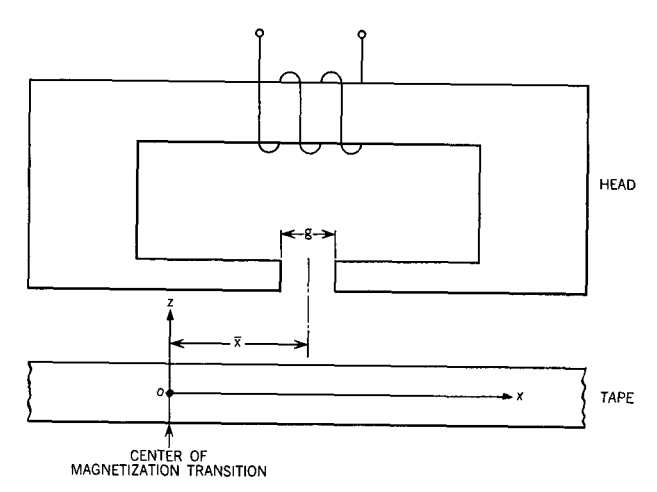


Figure 11 Non-zero width transition with non-zero gap length head.

where
$$C_a = \left(\frac{d+\delta+a}{d+a}\right)^{0.02a}$$
,

giving a half pulse width of

$$(P.W.)_{50} = 2\sqrt{(d+\delta+a)(d+a)}.$$
 (26)

Equations (23) and (26), which include the effects of demagnetization, may be compared to Eqs. (14) and (17) derived in the absence of demagnetization. It is enlightening to note the effect of the spreading of the transition region upon the calculations for the amplitude and readback pulse width. By contrast, the application of the reciprocity theorem to this case⁶ results in a much more complicated expression which does not afford this insight.

• The reproduced pulse by non-ideal ring transducer for a magnetization transition of non-zero width

This is the general case, shown schematically in Fig. 11. The flux $d\Phi_e$ linking the read coil will be only a fraction of the total flux $d\Phi$ emanating from the surface, ^{12,13}

$$d\Phi_c = \frac{R_2}{R_1 + R_2} d\Phi,$$

where R_2 is the reluctance of a flux path through the gap and R_1 is the reluctance of a flux path through the coil. The following two cases are distinguished;

(a) For
$$0 \le x \le \bar{x} - \frac{g}{2}$$
,

$$R_1 = R_c$$
 and $R_2 = gr_a$,

where R_o is the core reluctance and r_o is the gap reluctance per unit length.

(b) For
$$\bar{x} - \frac{g}{2} \le x \le \bar{x} + \frac{g}{2}$$
, $R_1 = R_c + r_o \left(x - \bar{x} + \frac{g}{2} \right)$ and

$$R_2 = r_g \left(\bar{x} + \frac{g}{2} - x \right).$$

Using the head sensitivity factor,

$$\alpha = \frac{gr_g}{gr_g + R_c},$$

the total flux linking the read coil becomes

$$\Phi_c = \alpha W \left[\int_0^{\bar{x}-g/2} B_z \left(x, d + \frac{\delta}{2} \right) dx + \int_{\bar{x}-g/2}^{\bar{x}+g/2} \frac{\bar{x} + \frac{g}{2} - x}{g} B_z \left(x, d + \frac{\delta}{2} \right) dx \right],$$

where $B_z(x, d + \delta/2)$ is given by Eq. (21).

Integrating this equation and differentiating with respect to time, we have, by analogy to Eqs. (22) and (23),

$$e(\bar{x}) = \left[Nv W\alpha (I_r \times 10^{-8}) \frac{4\mu}{\mu + 1} \cdot \frac{1}{g} \right]$$

$$\times \left[\left(\bar{x} + \frac{g}{2} \right) \log \frac{\left(\bar{x} + \frac{g}{2} \right)^2 + (d + \delta + a)^2}{\left(\bar{x} + \frac{g}{2} \right)^2 + (d + a)^2} \right.$$

$$- \left(\bar{x} - \frac{g}{2} \right) \log \frac{\left(\bar{x} - \frac{g}{2} \right)^2 + (d + \delta + a)^2}{\left(\bar{x} - \frac{g}{2} \right)^2 + (d + a)^2}$$

$$+ 2(d + \delta + a) \left\{ \tan^{-1} \frac{\bar{x} + \frac{g}{2}}{d + \delta + a} \right\}$$

$$- \tan^{-1} \frac{\bar{x} - \frac{g}{2}}{d + \delta + a} \right\}$$

$$- 2(d + a) \left\{ \tan^{-1} \frac{\bar{x} + \frac{g}{2}}{d + a} - \tan^{-1} \frac{\bar{x} - \frac{g}{2}}{d + a} \right\}.$$
(27)

Equation (27) defines the shape and amplitude of the reproduced pulse for the most general case. From this, one can easily determine the maximum value of the pulse $e_{\text{max}} = e(0)$, and the pulse width at any percent of the peak amplitude.

Again, comparing this equation with Eqs. (14) and (23), one can see how each individual parameter affects the signal amplitude and the resolution of a recording system. The reciprocity theorem has not been extended to include analytically the effect of the playback gap, except by harmonic analysis.

Experimental verification

The half pulse width reproduced by an ideal transducer is given by Eq. (26):

$$(P.W.)_{50} = 2\sqrt{(d+\delta+a)(d+a)}.$$

For thin recording surfaces,

$$d + a \gg \delta$$

and a binomial expansion of Eq. (26) gives:*

$$(P.W.)_{50} \approx 2(a+d) + \delta. \tag{28}$$

Similarly, from Eq. (24), the pulse amplitude is

$$e_{\max} \approx I_r \log \frac{d+\delta+a}{d+a} = I_r \log \left(1 + \frac{\delta}{d+a}\right).$$

For thin recording surfaces,

$$d + a \gg \delta$$
, and $\log \left(1 + \frac{\delta}{d+a}\right) \approx \frac{\delta}{d+a}$.

Therefore,

$$e_{max} \approx I_{r}\delta/(d+a)$$
.

If we assume $d \ll a$ we obtain $e_{max} \approx I_r \delta/a$, and since $a \approx (I_r \delta/H_c)^{\frac{1}{2}}$ we have

$$e_{\max} = (I_r \delta H_c)^{\frac{1}{2}}. \tag{29}$$

The half pulse widths calculated from Eq. (28) are in very close agreement with those calculated from Eq. (27) for a high resolution read gap (g=40 microinches). To evaluate Eq. (27) we need first to determine a value for the transition region parameter a. The slope at the origin of the assumed magnetization transition function

$$I_x = \frac{2}{\pi} I_r \tan^{-1} \frac{x}{a}$$

is $2/\pi$ (see Fig. 12), and consequently we can write as an approximation:

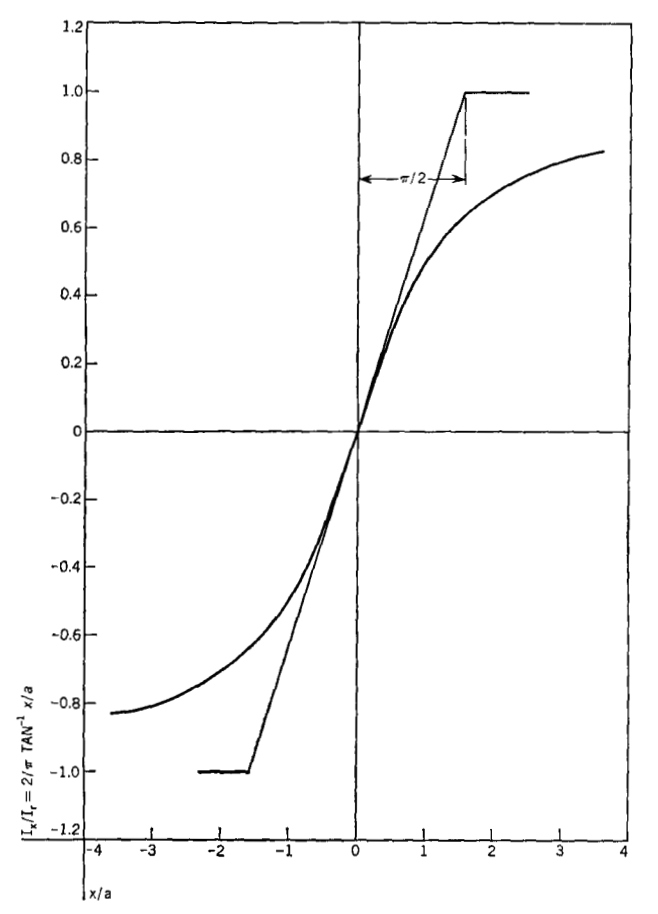


Figure 12 Definition of the magnetization transition region by the initial slope of the arctan function.

$$\frac{I_x}{I_x} = \frac{2}{\pi} \frac{x}{a}.$$

Extending this line to saturation $(I_x/I_r = 1)$ we get:

$$a = \frac{2}{\pi}x\tag{30}$$

where the value of x is obtained from Eq. (9) by following the procedure used to calculate the resultant transition region $2x_0$ shown in Tables 1, 2, and 3. In the actual calculation, Eq. (9) was programmed in a computer to determine by a search the value of x_0 for values of H_x/I_r ranging from 0.01 to 2.00 with $\ell_0=25$ microinches (a reasonable value for thin surfaces) and δ as a parameter ranging from 2 to 30 microinches. The values of x_0 thus obtained were used as values of x in Eq. (30) to determine a, and the result inserted in Eq. 27 with d=30 microinches (a reasonable assumption for our recording system) and g=40 microinches to obtain the pulse shape, from which the half pulse width and the pulse amplitude were calculated. These theoretical results are shown in Figs. 13 and 14 along with some experimental results.

^{*} The linear appearance of Eq. (28) is perhaps somewhat misleading. In general, a and d are of the same order of magnitude, and whereas the half pulse width varies linearly with a, it does not vary proportionally to a. Therefore, if one wishes to establish a proportionality relationship between $(P.W.)_{50}$ and the magnetization transition region, the exponent in this relationship will depend on the relationship.

The experimental results were taken on a vacuum-column tape transport using a 36-inch loop of tape moving at a speed of 30 inches per second. The recording head had a write gap of 150 microinches and a read gap of 40 microinches. As recording surfaces we used metallic films of different compositions and thicknesses. The range of magnetic properties and thicknesses used was:

$$H_c = 15-1200 \text{ Oe}, \qquad \delta = 3-35 \text{ microinches},$$

 $I_r = 300-1000 \text{ emu/cc}.$

The recording surfaces were ac-erased prior to recording on NRZI pattern at 100 bits per inch using a square wave generator. This bit density is low enough to avoid interaction effects, and allowed us to photograph on an oscilloscope an essentially isolated pulse and determine its amplitude and its width at the half amplitude point. The writing transducer current was adjusted for optimum read pulse amplitude—not a critical adjustment for thin recording surfaces.

In Fig. 13 the abcissa is the ratio of the coercivity to the thickness of the recording surface. We chose this ratio because it provides the best experimental correlation.¹⁴

The reason that I_r does not significantly affect the half pulse width of the read-back pulse is believed to be related to the slope of the magnetization transition, which is equivalent to the magnetic charge density in the transition region. From Eq. (30) the linearized transition region is πa , and from Eq. (11)

$$a \propto \left(\frac{I_r \delta}{H_c}\right)^{\frac{1}{2}}$$
.

If, for example, we double I_r , the transition region increases by the factor $\sqrt{2}$, and the same effect is observed if we decrease H_c by a factor of 2. However, in the former case, the slope of the magnetization in the transition region also increases by the factor $\sqrt{2}$, whereas in the latter case the slope decreases by $\sqrt{2}$. Thus, increasing I_r or decreasing H_c by the same factor produces an identical effect in lengthening the transition region, but results in much different magnetization transition slopes. The larger slope resulting from an increase in I_r partly compensates for the corresponding widening of the transition region.

The assumption of an arctan function or a linearization of the transition region is an oversimplification. The demagnetizing field is zero at the center of the transition region, increases to a maximum at some distance from the center, and decreases gradually thereafter. Consequently, a certain region about the center will not be affected by demagnetization; the result is a very sharp slope for the magnetization at the center of the transition region. Beyond this, a more gradual slope appears because of demagnetization effects. It is believed that expressing

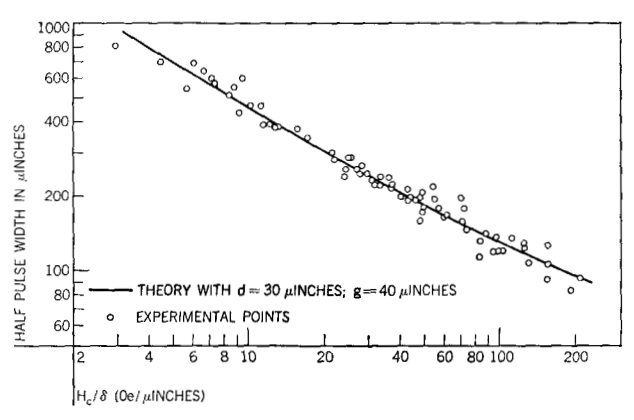
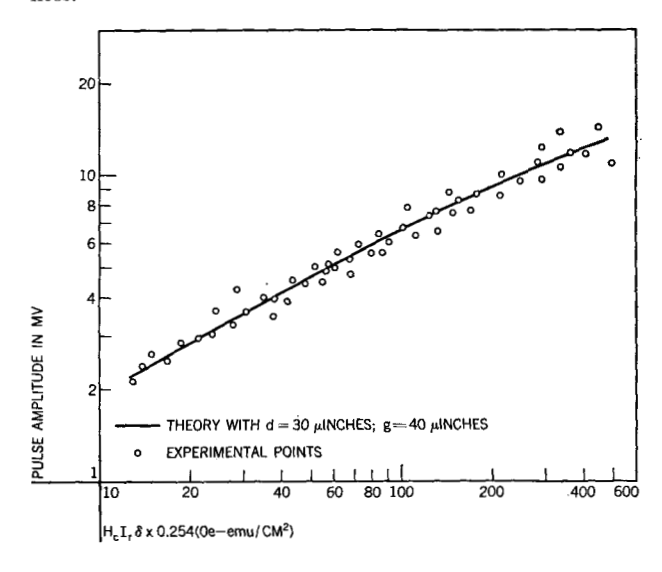


Figure 13 The 50% pulse width vs the coercivity-to-thickness ratio of the recording surface.

Figure 14 Maximum pulse amplitude vs product of coercivity, remanent magnetization and recording surface thickness.



the transition region by the initial slope of the arctan function is, in effect, averaging the two different slopes of the actual magnetization distribution. A more exact calculation is to be published.

The agreement of the theory with experiment is indeed excellent. Furthermore, it is quite apparent from Figs. 13 and 14 that, over this extensive range of magnetic parameters and recording surface thickness,

$$(P.W.)_{50} \propto \left(\frac{H_c}{\delta}\right)^{-1/2},$$
 (31)
 $e_{\text{max}} \propto (H_c I_r \delta)^{1/2}.$

242

These proportionality relations are in excellent agreement with our experimental findings. 1,14

Conclusions

The equations developed above describe the demagnetization of non-interacting recorded transitions, and the characteristic width and amplitude of the pulse read-back from such transitions. These equations enable one to determine the effect of each of the magnetic and recording parameters on the resolution and signal output of a recording system. It has been shown that the writing process plays a minor role, particularly in thin recording surfaces. On the other hand, demagnetization is very important, which strongly implicates the magnetic parameters and the thickness of the recording surface in the resolution and amplitude of the read-back pulse. Also, the transducer-to-medium spacing and the read gap are very important parameters; their relative effects depend on their relative magnitudes. Any one of these three parameters-transition region length, transducer to medium spacing, and read gap length-can dominate the pulse width, depending on its size relative to the others.

The theoretical predictions are in excellent agreement with experimental measurements on a large number of thin recording surfaces with widely different properties.

References

- D. E. Speliotis, J. R. Morrison, J. S. Judge, *IEEE Trans. Mag.* MAG-1, 348 (1965).
- 2. A. Aharoni and R. D. Fisher, Proc. INTERMAG 1965, 12.3-1.
- A. V. Davies, B. K. Middleton, A. C. Tickle, *IEEE Trans. Mag.* MAG-1, 344 (1965).
- 4. W. K. Westmijze, *Philips Res. Rep.* 8, 148–157, 161–183, 245–269, 343–366 (1953).
- A. S. Hoagland, Communications and Electronics (AIEE), 75, 506 (1956).
- 6. D. F. Eldridge, IRE Trans. Audio AU9, 42 (1960).
- 7. K. Teer, Philips Res. Rep. 16, 469 (1961).
- 8. G. Y. Fan, IBM Journal 5, 321 (1961).
- J. J. Miyata and R. R. Hartel, IRE Trans. Elect. Comp. EC-8, 159 (1959).
- 10. D. W. Chapman, Proc. IEEE 51, 394 (1963).
- 11. R. L. Wallace, Jr., Bell Sys. Tech. Journ., 30, 1145 (1951).
- E. D. Daniel and P. E. Axon, *Proc. IEE* 100, Part III, 157 (1953).
- M. Nishikawa, El. Com. Lab. Tech. Journ. (Nippon) 12, 249 (1963).
- 14. D. E. Speliotis, J. R. Morrison and J. S. Judge, presented at the International Conference on Nonlinear Magnetics (INTERMAG), April 20–22, 1966.
- J. Hokkyo, "Theoretical Analysis of Digital Recording Mechanism and the Limit of Recording Density," presented to the Magnetic Recording Institute, Electrical Communication Engineers, Tokyo, Japan, November 25, 1965 (to be published).

Received December 3, 1965.